High cycle multiaxial fatigue crack initiation : experimental observations and microstructure simulations

K. AGBESSI[a*], N. SAINTIER[a], T. PALIN-LUC[a]

a. *Arts et Métiers ParisTech, I2M, CNRS, Université de Bordeaux, Esplanade des Arts et Métiers, F-33405 Talence, France*

Résumé :

Cette tude propose une analyse des modes d'amorage de fissures en fatigue multiaxiale grande dure de vie en se basant principalement sur des observations MEB. L'tude statistique des sites prfrentiels d'amorage de fissures montre que les grains glissement multiple prsentent une forte probabilit d'amorage de fissures. L'application du critre de Dang Van l'chelle des grains grce des calculs par lments finis (lasticit cubique avec/sans plasticit cristalline) sur des microstructures synthtiques 3D semi-priodiques montre une forte htrognit de la contrainte hydrostatique et du cisaillement. L'volution de cette htrognit en fonction du type de comportement introduit dans le calcul est discute. Enfin, une mthode base sur la statistique des valeurs extrmes est propose pour dpouiller les calculs sur agrgats et est applique la contrainte quivalente associe au critre de fatigue de Dang Van. Les effets de surface libre et du modle de comportement ont t analyss.

Abstract :

This study provides an analysis of high cycle multiaxial fatigue crack initiation modes based on SEM observations. The statistical study of crack initiation preferential sites shows that grains with multiple slip have a high probability of crack initiation. The application of Dang Van criterion at the grain scale using finite element analysis (cubic elasticity with / or without crystal plasticity) on 3D synthetic semi-periodic microstructures shows a strong heterogeneity of both the hydrostatic stress and shear. The evolution of this heterogeneity introduced by the material behavior is discussed. Finally, a method based on the extreme values statistics is proposed and applied to the fatigue indicative parameter associated to the Dang Van criterion. The effects of free surface and constitutive material model were analyzed.

Keywords : high cycle multiaxial fatigue ; crack initiation ; extreme value statistic

1 Introduction

After several decades of research in the field of fatigue of materials and structures [1, 2], the current criteria have reached a certain maturity and allow scientists and engineers to understand many service situations efficiently. Although there is no unified approach for all real situations that may occur on a structure or for all classes of materials, current approaches have a wide spectrum of applications. In most cases, such approaches allow efficient structure design against fatigue crack initiation on metallic materials. The vast majority of methods for high cycle fatigue (HCF) life assessment are based on mechanical quantities calculated at macroscopic or mesoscopic scale. Most of these methods found in the literature are based on assumptions at the mesoscopic scale of the material's polycrystalline plasticity among which Dang Van [3] or Papadopoulos [4] approaches widely used in industry. Although different levels of damage mechanisms involved in the process of HCF crack initiation are relatively well identified (grain scale and slip bands [5]) very few models take into account explicitly the exact nature of these mechanisms. The aims of this study is to better understand the role of microstructure in the process of HCF crack initiation under complex loading conditions so as to allow their integration into multiaxial HCF criteria sensitive to microstructure.

2 Experimental procedures

An OFHC (Oxygen Free High Conductivity) pure copper (99.99%) has been used in this study. The material is supplied in the form of rectangular hot rolled plate. An annealing relaxation treatment of 230°C during 1h was performed. The grains are equiaxed with an average diameter of 35 μm. The material has a isotropic texture with a texture index of 1.05. The fatigue tests were carried out in air, at room temperature, under fully reversed loadings (tension, torsion and combined tension-torsion) at a frequency f = 20 Hz on cylindrical smooth specimens. The specimen surface was observed after 10^6 cycles without macroscopic failure under loading conditions corresponding to the median fatigue limit at 10^6 cycles (see Table 1).

TABLE 1 – Different applied loading conditions corresponding to the median fatigue limit at 10^6 cycles.

Loading conditions	σ_a [MPa]	τ_a [MPa]	σ_a/τ_a	β [0°]
Tension (σ_a)	85	-	-	-
Torsion (τ_a)	-	58	-	-
Tension-torsion ($\sigma_a/\tau_a = 2.0(0^o)$)	68	34	2.0	0
Tension-torsion ($\sigma_a/\tau_a = 0.5(0^o)$)	24	48	0.5	0
Tension-torsion ($\sigma_a/\tau_a = 2.0(45^o)$)	68	34	2.0	45
Tension-torsion ($\sigma_a/\tau_a = 0.5(45^o)$)	24	48	0.5	45
Tension-torsion ($\sigma_a/\tau_a = 2.0(90^o)$)	68	34	2.0	90
Tension-torsion ($\sigma_a/\tau_a = 0.5(90^o)$)	24	48	0.5	90

3 Micro-mechanical modeling

3.1 Material mechanical behavior

In this work, the crystal plasticity constitutive model proposed by Meric and Cailletaud [6] is used for polycrystalline aggregates computations. The constitutive equations of the model are written in the framework of crystal plasticity taking into account both the isotropic and kinematic hardening on the slip systems. It is a time dependent crystal plasticity model with the assumption of small perturbations. The shear strain rate $\dot{\gamma}^s$ on the slip system s is described by a power function :

$$\dot{\gamma}^s = \left\langle \frac{|\tau^s - x^s| - r^s}{K} \right\rangle^n \text{sign}(\tau^s - x^s) \text{ with } \langle x \rangle = \left\{ \begin{array}{c} x \text{ if } x \geq 0 \\ 0 \text{ if } x \leq 0 \end{array} \right\} \tag{1}$$

where K and n are material parameters describing the viscosity. The evolution of the isotropic and kinematic hardening are non linear.

$$r^s = R_o + Q \sum_s h_{sr}(1 - e^{-b\upsilon^s}) \tag{2}$$

where τ_o is the initial critical resolved shear stress, Q and b represent respectively the capacity and speed of isotropic hardening and $\underline{\underline{h}}$ describe the slip systems interactions. υ^s is so that $\dot{\upsilon}^s = |\dot{\gamma}^s|$.

$$x^s = c\alpha^s \text{ with } \dot{\alpha}^s = \dot{\gamma}^s - d\alpha^s\dot{\upsilon}^s \tag{3}$$

where c/d and d describe respectively the capacity and speed of kinematic hardening.

TABLE 2 – Material parameters identified for pure OFHC copper.

Viscosity		Isotropic hard.			Kinematic hard.		Interaction matrix					
K	n	R_o [MPa]	Q [MPa]	b	c [MPa]	d	h_o	h_1	h_2	h_3	h_4	h_5
8	20	13	9	33	2000	960	1	1	0.2	90	3	2.5

The material parameters (cf. table 2) are identified form experimental cyclic hardening curves under constant total strain rate of $\dot{\varepsilon} = 3.2.10^{-3}\ s^{-1}$ using the half-life stabilized hysteresis loop. Parameters describing the viscosity and the interaction matrix between slip systems are not identified but chosen identical to those identified by Grard [7] on pure copper. The anisotropic elasticity constants suggested in [6] have been used. Indeed,

$C_{11} = 151\,\text{GPa}$; $C_{12} = 121.9\,\text{GPa}$; $C_{44} = 80.9\,\text{GPa}$ (Voigt notation). Numerical and experimental stabilized cyclic behavior are compared on Figure 1. There is a good agreement between model and experiments especially for low strain amplitudes corresponding to HCF domain.

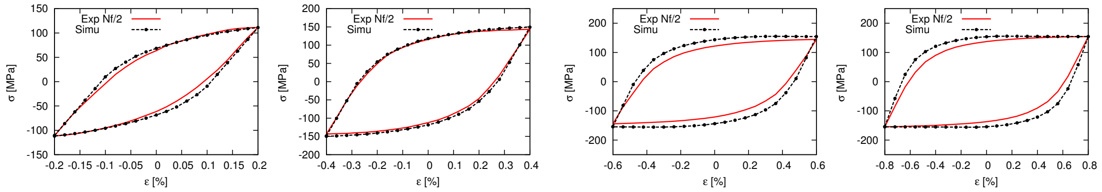

(a) $\varepsilon = \pm 0.2\%$ (b) $\varepsilon = \pm 0.4\%$ (c) $\varepsilon = \pm 0.6\%$ (d) $\varepsilon = \pm 0.8\%$

FIGURE 1 – Stabilized hysteresis loops numerical ("Simu") and half-life experimental ("Exp Nf/2") ones.

3.2 Strategy and finite element computations

The size of the representative element volume (REV) is defined in terms of the mechanical behaviour of a material in order to accurately reflect its macroscopic behavior. The size of the REV depends on the considered phenomenon. The definition of the REV size, in terms of it constitutive behaviour is different in terms of fatigue. The process of fatigue crack initiation is not a grain average type response. Cracks are initiated mostly in "critical" grains whose orientation, morphology and other parameters (neighbouring grain effects, free surface effects, etc.) create favourable conditions. Thus, the size of a REV in regards to fatigue can be very large, to the point that the computational tools currently available are not capable of undertaking the calculation [8]. The methodology consists of constructing a set of numerical elementary volumes (representative in terms of the monotonic/cyclic macroscopic behavior) so as to reproduce a statistical response that is representative of the structure with respect to the phenomenon of crack initiation. Each of these elementary volumes is a microstructure sample (in terms of statistics) and will be called SEV (statistical elementary volumes). Each SEV contains 200 grains (cf. figure 2), which allows the calculations to be done in sequential mode without parallel processing. Several calculations were performed in order to have statistically representative results using 7 different semi-periodic SEV and 5 sets of random orientations (i.e. isotropic texture). Periodicity is ensured in 2 directions (X and Y) where semi-periodic stress boundary conditions are applied. For each SVE, the macroscopic behavior is stable. Two material behaviors are considered : cubic elasticity (EL) with 30 calculations per loading conditions and cubic elasticity + crystal plasticity (PC) with 20 calculations per loading conditions. The applied loadings are those applied experimentally and corresponding to the experimental median fatigue limit of the material at 10^6 cycles (see Table 1).

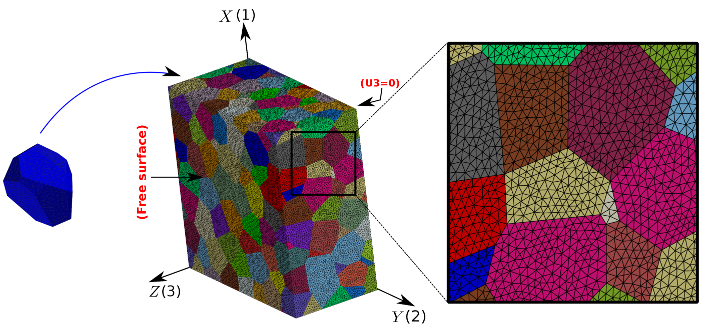

FIGURE 2 – 3D semi-periodic microstructure with 200 grains (about 50 grains on the free surface). About 500,000 elements and 300,000 degrees of freedom.

4 Results et discussions

4.1 Fatigue crack initiation

Figure 3a represent the proportion of grains according to the different modes of crack initiation for each loading conditions. In tension, we note that the cracks often initiate at the grain boundaries (about 57 % of cases). Grain boundaries seems to facilitate the localization of plastic deformation under tension loading. Strain incompatibilities at grain boundaries seem to play a significant role in the development of HCF damage in tension. In the case of torsion, where PSB grow more evenly in several grains, the proportion of crack initiation at grain boundaries is 40% (17 points less compared to tension). In this case, plastic activity inside the grain dominates the activity at the grain boundary. For all the loading cases investigated, the majority of observed cracks are initiated within the grains with a single slip system activated visible. The proportion of cracks initiated at grain boundaries is about 40%. An amount of about 10% of the grains with at least two visible activated slip systems is observed. It is clear from this analysis that the HCF crack initiation is mainly intragranular on OFHC copper studied. The percentage of crack initiation in grains with multiple slip is relatively low. However, the effect of grain boundaries (including twin boundaries) is important. Focusing only on intragranular crack initiation, we can also establish a link between the plastic activity in terms of number of activated slip systems and the modes of crack initiation in the grains. The proportion of intergranular crack initiation over the percentage of grains with single slip and multiple slip is analyzed. Let us note P_{ss} the percentage of grains with single slip and P_{ms} with the multiple slip. One can define the percentage of grains with intragranular crack initiation reported to the percentage of grains with PSB (plastic slip) by $P_{is/ss} = \frac{P_{is}}{P_{ss}}$ and $P_{im/ms} = \frac{P_{im}}{P_{ms}}$ where P_{is} et P_{im} are respectively the percentage of grains with intragranular crack initiation in single slip and multiple slip grains. Intragranular crack initiation occurs mostly in grains with single slip (see Figure 3b) for all the loading conditions investigated. However, non-proportional multiaxial and torsion loading conditions induce high probability of crack initiation on multiple slip grains. These grains are also vulnerable to crack initiation in the same way as grains with single slip for these non-proportional multiaxial loading conditions.

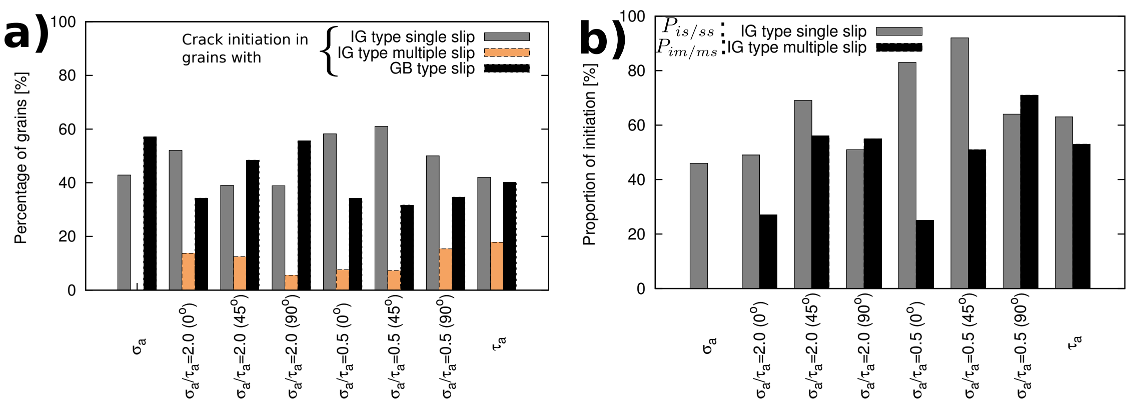

FIGURE 3 – (a) Proportion of intragranular crack initiation (in grains with one and at least two visible activated slip systems) and intergranular (at grain boundary). (b) Proportion of intragranular crack initiation with regard to the percentage of grains with single and multiple slip. Approximately 60 grains were considered for each loading conditions.

4.2 Extremes values statistic

Critical grain of the microstructure (in which cracks are likely to initiate) according to the Dang Van criterion are those that maximize the fatigue indicator parameter (FIP), noted I_{DV} (eq. (4)). The Dang Van FIP is computed for each grain considering its local stress state (obtained by FE analysis) and its orientation. The planes and the directions on which the criterion is evaluated correspond to the slip systems of the grain. We propose in this section, an analysis of the extreme values of I_{DV}.

$$I_{DV} = \max_{s=1,\dots,12} \left\{ \max_{t} [\| \underline{\tau}(s,t) \| + \alpha_{DV} \sigma_H(t)] \right\} \leq \beta_{DV} \tag{4}$$

where $\sigma_H(t) = \frac{1}{3} trace(\underset{\sim}{\boldsymbol{\sigma}}(t))$ represent the hydrostatic stress. $\| \underline{\tau}(s,t) \|$ denotes the centered resolved shear stress for each slip system s, by constructing the smallest circle circumscribing the loading path. This resolved shear stress is computed using the averaged stress tensor $\underset{\sim}{\boldsymbol{\sigma}}$ in the grain. At the grain scale, significant variability was observed for the hydrostatic stress and shear, as it was recently shown in the case of 2D polycrystalline aggregates computations [9].

4.2.1 Generalized extreme values probability

As given a random variable X with distribution function $F_X(x)$, the overall n extreme values of the variable X can be defined as $Y_n = \max(X_1, X_2, ...X_n)$ and the cumulative probability function F_{Y_n} is linked to F_X by $F_{Y_n}(x) = [F_X(x)]^n$. As proposed by the Fisher-Tippet theorem, if there are two normalizing real sequences $(a_n)_{n\geq 1} > 0$ and $(b_n)_{n\geq 1}$ and a non-degenerate distribution (not reduced to one point), $G(x)$ so that

$$P\left(\frac{Y_n - b_n}{a_n} \leq x\right) = [F(a_n x + b_n)]^n \underset{n\mapsto +\infty}{\longrightarrow} G(x) \tag{5}$$

then the generalized extreme value (GEV) distribution function can be written as the following unique equation [10] :

$$G_\xi(x) = \begin{cases} \exp\left(-(1+\xi x)^{-\frac{1}{\xi}}\right) & \text{if } \xi \neq 0, \forall x \,/\, 1+\xi x > 0 \\ \exp(-\exp(-x)) & \text{if } \xi = 0 \end{cases} \tag{6}$$

The sign of the extreme index ξ indicates the attractive domain of the extreme values ($\xi = 0$ for Gumbel, $\xi > 0$ for Frchet and $\xi < 0$ for Weibull). This allows us to determine the best extreme value distribution function represent the extreme values of X and not to choose a priori a given type of distribution function.

4.2.2 Free surface effects

The median thresholds of Dang Van criterion at the mesoscopic scale are compared in Figures 4a-b. The free surface causes a decrease of the mechanical quantities (shear and normal stress) associated to the criterion. In the case of cubic elasticity behavior only, the macroscopic criterion threshold is identical to the mesoscopic one considering the free surface only. For the grains in the volume of the microstructure, the mesoscopic criterion threshold is shifted upwards compared to the macroscopic one. This shift comes mostly from the strong variation of the hydrostatic stress. The extreme values of the volume grains gives a higher median value of I_{DV} and in the ranges of greater hydrostatic stress compared to the free surface grains. The same results are obtained for cubic elasticity + crystal plasticity behavior. It should be noted that in this case, the median mesoscopic criterion threshold with the free surface grains is below the macroscopic one.

4.2.3 Material behavior effects

Whether the free surface or the volume of the aggregate, one can see on Figures 4c-d, that cubic elasticity alone leads to extreme values higher than when coupled with crystal plasticity. The elastic anisotropic has important effect compare to the crystal plasticity. Thus, taking into account the crystal plasticity constitutive law reduces shear and normal stress. This effect is also more pronounced in volume grains compared the free surface ones for the same material behavior. This seems to come from the important neighboring effect in grains located in the volume where the grains are confined. Due to higher hydrostatic stress, grains located in the volume seems to be more critical than those on the free surface. This is different from experimental observations but may be related to the definition of the free surface (for instance the number of grains in the thickness of the aggregates). Furthermore, roughness of the real surface is not considered in our calculations.

5 Conclusion

Different modes of high cycle fatigue microcracks initiation were observed under complex loading conditions at stress levels close to the median fatigue limit of the material at 10^6 cycles. SEM observations showed that, for the studied material, non-proportional loading conditions induce an increase of the probability of crack initiation in multiple slip grains. The multiple slip plays a considerable role in the process of crack initiation under these loading. However, in general for all loading cases studied, the probability of microcracks initiation in the single slip grains is the highest. From the finite element computations of polycrystalline aggregates, it can be conclude that the heterogeneity of the hydrostatic stress and shear is mainly due to the elastic anisotropic behavior. The small effect of plasticity is probably due to the low stress levels applied (corresponding to the median fatigue limit at 10^6 cycles) with small plastic strain amplitude. The sensitivity of the microstructure in multiaxial fatigue was explored by performing simulation of multiple statistic volume elements and showing

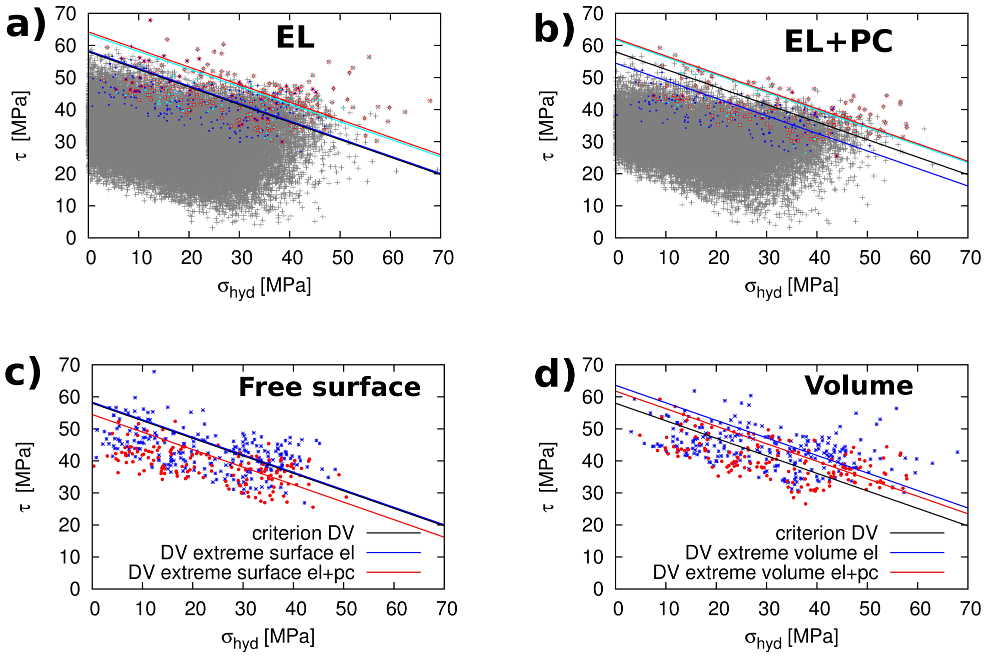

FIGURE 4 – (a,b) Comparison of extreme values plotted with "dark blue", "red" and "light blue " corresponding respectively to the extreme values obtained by considering only the free surface, the entire microstructure and the volume. (c,d) Comparison of the extreme values obtained with cubic elasticity alone ("el") and cubic elasticity + crystal plasticity ("el+pc").

the effects of the free surface and the constitutive model on the fatigue indicator parameter associated to the Dang Van criterion. The results provide interesting insights into the multiaxial fatigue modeling of metals and structures taking into account the microstructure.

Références

[1] J. Schijve. Fatigue of structures and materials in the 20th century and the state of the art. *International Journal of Fatigue.*, 25 :679–702., 2003.

[2] A. Fatemi and N. Shamsaei. Multiaxial fatigue : An overview and some approximation models for life estimation. *International Journal of Fatigue*, 33 :948 – 958, 2011.

[3] K. Dang-Van, G. Cailletaud, J.-F. Flavenot, L. Douaron, and H.-P. Lieurade. Criterion for high-cycle fatigue failure under multiaxial loading. *In Biaxial and Multiaxial Fatigue (Sheffiled)*, pages 459–478, 1989. M. Brown and K. Miller, Eds.

[4] I. Papadopoulos. A new criterion of fatigue strengh for out-of-phase bending and torsion of hard metals. *International Journal of Fatigue.*, 16 :377–384., 1994.

[5] A. Trochidis, E. Douka, and B. Polyzos. Formation and evolution of persistent slip bands in metals. *Mechanics and Physics of Solids.*, 48 :1761–1775, 2000.

[6] L. Meric and G. Cailletaud. Single crystal modeling for structural calculations : Part 2 - finite element implementation. *Journal of Engineering Materials and Technology*, 113(1) :171–182, 1991.

[7] C. Gerard. *Mesures de champs et identification de modèles de plasticité cristalline*. PhD thesis, Université Paris 13, France, 2008.

[8] C. Przybyla, R. Prasannavenkatesan, N. Salajegheh, and D. L. McDowell. Microstructure-sensitive modeling of high cycle fatigue. *International Journal of Fatigue*, 32(3) :512 – 525, 2010.

[9] C. Robert, N. Saintier, T. Palin-Luc, and F. Morel. Micro-mechanical modelling of high cycle fatigue behaviour of metals under multiaxial loads. *Mechanics of Materials*, 55(0) :112 – 129, 2012.

[10] A.F. Jenkinson. The frequency distribution of the annual maxima (or minimum) values of meteorological elements. *Quaterly Journal of the Royal Meteorological Society*, 81, 1955.